DISTRIBUTION STATEMENT A. Approved for public release; distribution is unlimited.

Variable Resolution Dynamical Cores with Full Physics

Saša Gaberšek
Naval Research Laboratory
7 Grace Hopper Avenue, Stop 2
Monterey, CA 93943-5502
phone: (831) 656-4882 fax: (831) 656-4769 email: sasa.gabersek@nrlmry.navy.mil

Award Number: N0001412WX20684
http://faculty.nps.edu/fxgirald/projects/NUMA
http://www.nrlmry.navy.mil/projects/coamps

LONG-TERM GOALS

The long-term goal of this project is to maintain the leading edge of the Numerical Weather Prediction (NWP) models by improving the existing US Navy mesoscale atmospheric forecast model, the Coupled Ocean/Atmosphere Mesoscale Prediction System (COAMPS®[1]) and, at the same time continue developing the next generation model with an ability for prediction across spatial and temporal scales.

OBJECTIVES

There are two main objectives, one for each target. First, to continue development of the next generation model, the Spectral Element (SE) model, built on the Element Based Galerkin (EBG) method and evaluate detailed simulations in two-dimensions (2D) and preliminary tests in three dimensions (3D). The primary focus is on adding physical parameterizations, with some effort directed toward the model infrastructure.

Second, to improve the current generation version of COAMPS by implementing a recently developed implicit damping in the top sponge layer for stability purposes. The overarching objective is to develop a dynamical core suitable for the unified approach in support of NWP.

APPROACH

The major thrust in our effort is aimed at the development of the SE model, leveraged by improvements of COAMPS.

1. SE Model

   We will adhere to best coding standards while working on the SE model source code infrastructure. There needs to be a clear separation of physical parameterizations and the dynamical core of the model. We will develop a module which will contain all relevant pieces of the code for the subgrid-scale mixing, based on the K-theory. The mixing will be tested on

[1] COAMPS® is a registered trademark of the Naval Research Laboratory.

idealized cases, both in two- and three-dimensions. In addition, the implementation of physical parameterizations needs to be accessible to future developers not familiar with the SE model. A separate module containing all differential operators specific for the SE model will be written and the rest of the source code modified to include it.

2. COAMPS

   The information leaving the computational domain (e.g. waves) should not be reflected inwards at the domain boundaries. For this purpose, there is a sponge layer at the top of the computational domain. The damping coefficient can impose a severe constraint on the maximum permitted time step to avoid instabilities, when damping is applied explicitly. One alternative approach is to apply it implicitly, which inherently relaxes the constraint, removes the instabilities and results in overall faster wall-clock time to complete a numerical simulation.

Key personnel: Saša Gaberšek (Naval Research Laboratory), P. Alex Reinecke (NRL), James D. Doyle (NRL), Dale R. Durran (University of Washington), Peter N. Blossey (UW), Francis X. Giraldo (Naval Postgraduate School), Jim. F. Kelly (NPS).

WORK COMPLETED

We have redesigned the source code of the SE model to accommodate a Fortran module containing all differential operators. We have ensured bit-by-bit reproducibility by comparing the results obtained with the original code for a linear, hydrostatic mountain wave.

We have implemented the physical parameterization of the subgrid-scale mixing, based on the K-theory (1st order closure), where K represents eddy diffusivity. The parameterization was tested on three cases: i) an elevated, two-dimensional jet in an isotropic atmosphere, ii) a two-dimensional, nonlinear flow over a ridge, and iii) a three-dimensional, nonlinear flow over an elongated mountain. The parameterization was tested over a limited subspace of the *h-p* parameter space, where *h* is the number of elements and *p* is the polynomial order.

The implicit damping in the sponge layer (Klemp et al, 2008) has been fully implemented in COAMPS and tested on the cases that were previously problematic (high latitude regions during the northern hemisphere winter).

RESULTS

During the implementation of the subgrid-scale mixing parameterization for the SE model we encountered an interesting problem. One of the parameters in the scheme, which determines the strength of mixing is a so called 'effective grid scale'. The choice is straight forward in models with a fixed grid, but in the SE model the nodal spacing (grid) varies within each element. Two obvious choices are i) node-specific grid scale and ii) element-averaged grid scale (Fig 1).

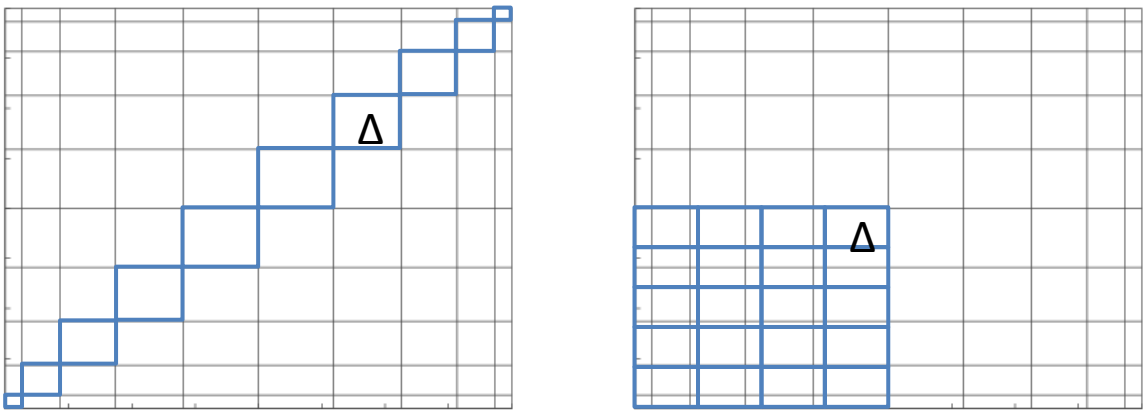

Figure 1: Choices for the effective grid scale (Δ), represented with blue rectangles for a portion of a typical element: node-specific (left panel) and element-averaged (right panel). Gray lines represent nodal points for the SE model using a 10th order polynomials for basis functions (p=10).

In addition, the mixing theory is based on isotropic turbulence, but the aspect ratio of horizontal to vertical grid spacing in most atmospheric models is far from unity. Thus, we tested an additional option, where the nodal spacing in vertical direction determines the effective grid scale.

The results of the SE model for the first test of an elevated jet with the subgrid-scale mixing parameterization suggest that the mechanical, shear-induced mixing in an atmosphere with a neutral stratification performs as expected – it is mixing momentum from the jet core into the regions with lower wind speeds (Fig 2).

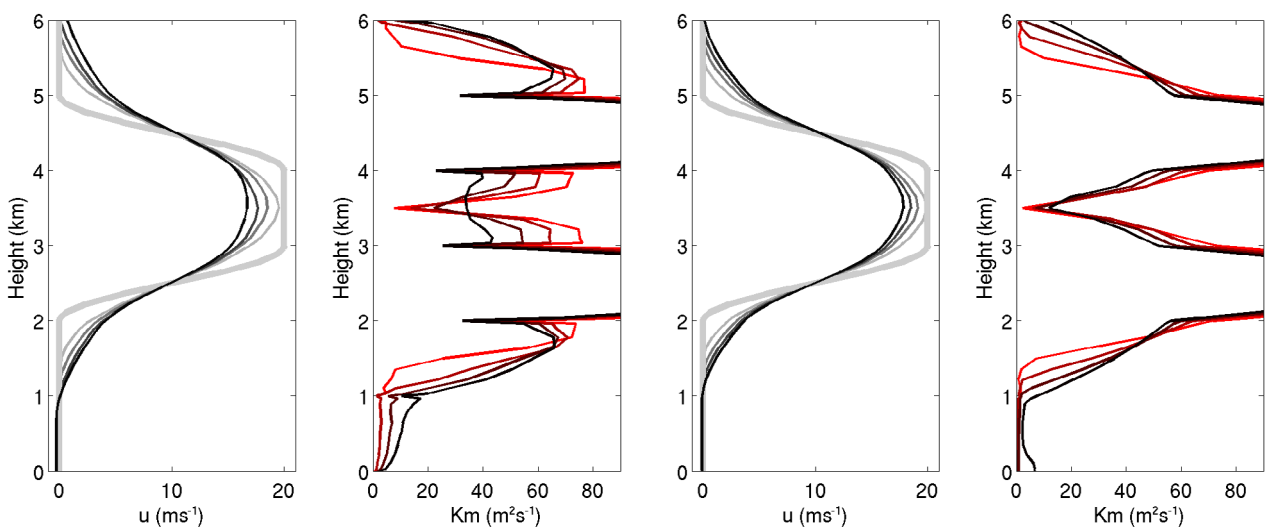

Figure 2: Wind speed (u) and mixing coefficient (Km) as a function of time for the node-specific (left two panels) and element-averaged (right two panels) effective grid scale (Δ). The initial profiles of the wind speed (mixing coefficient) are in light gray (light red), with darker shades representing the time evolution.

The second case represents a nonlinear flow over a ridge where the response of the flow results in significant mixing and wave breaking. We tested all four possible formulations for the effective grid scale (Fig 3). The most visible difference in the mixing coefficient occurs when the effective grid scale is determined by the vertical spacing of nodal points. The overall flow structure is otherwise very comparable.

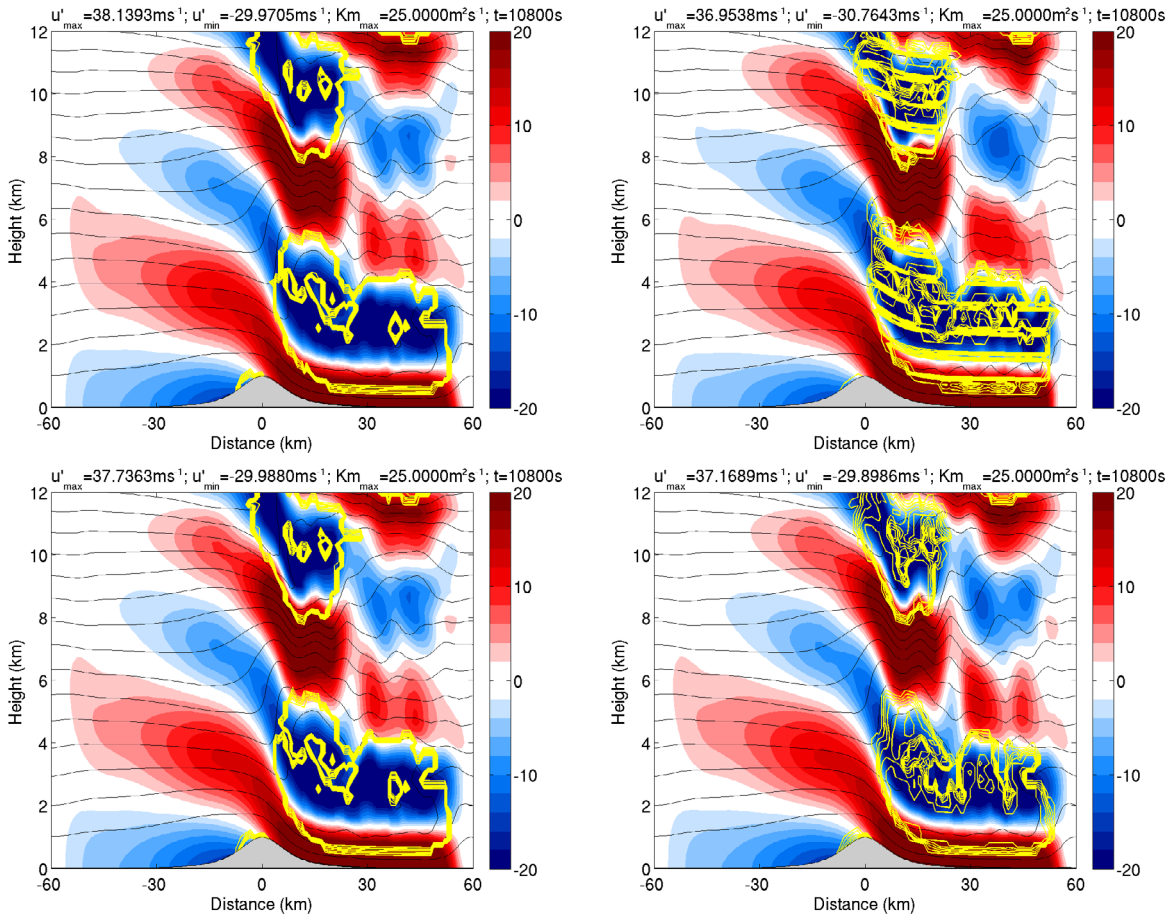

Figure 3: Perturbed u-component of the wind (filled contours, c.i. 2 ms^{-1}), potential temperature (black lines, c.i. 10 K), mixing coefficient (yellow contours, c.i. 5 m^{2}s^{-1}) and the mountain (gray). Plots are for the effective grid scale being node-specific (top left), node-specific, limited by the vertical nodal spacing (top right), element-averaged (bottom left) and element-averaged, limited by the average vertical nodal spacing (bottom right).

In addition to the sensitivity to the choice of the number of elements (*h*) and polynomial order (*p*), with the average grid spacing in both vertical and horizontal direction held constant ($<\Delta z>$=100 m, $<\Delta z>$=1000 m). The effective grid scale is node-specific, limited by the vertical nodal spacing. There aren't any significant differences across the *h*-*p* parameter space, except for a slightly weaker response and lack of mid-tropospheric trapped waves when using the lowest polynomial order (*p*=4). The out-of-phase difference can be explained by the fact that we are comparing snapshots in time (Fig 4).

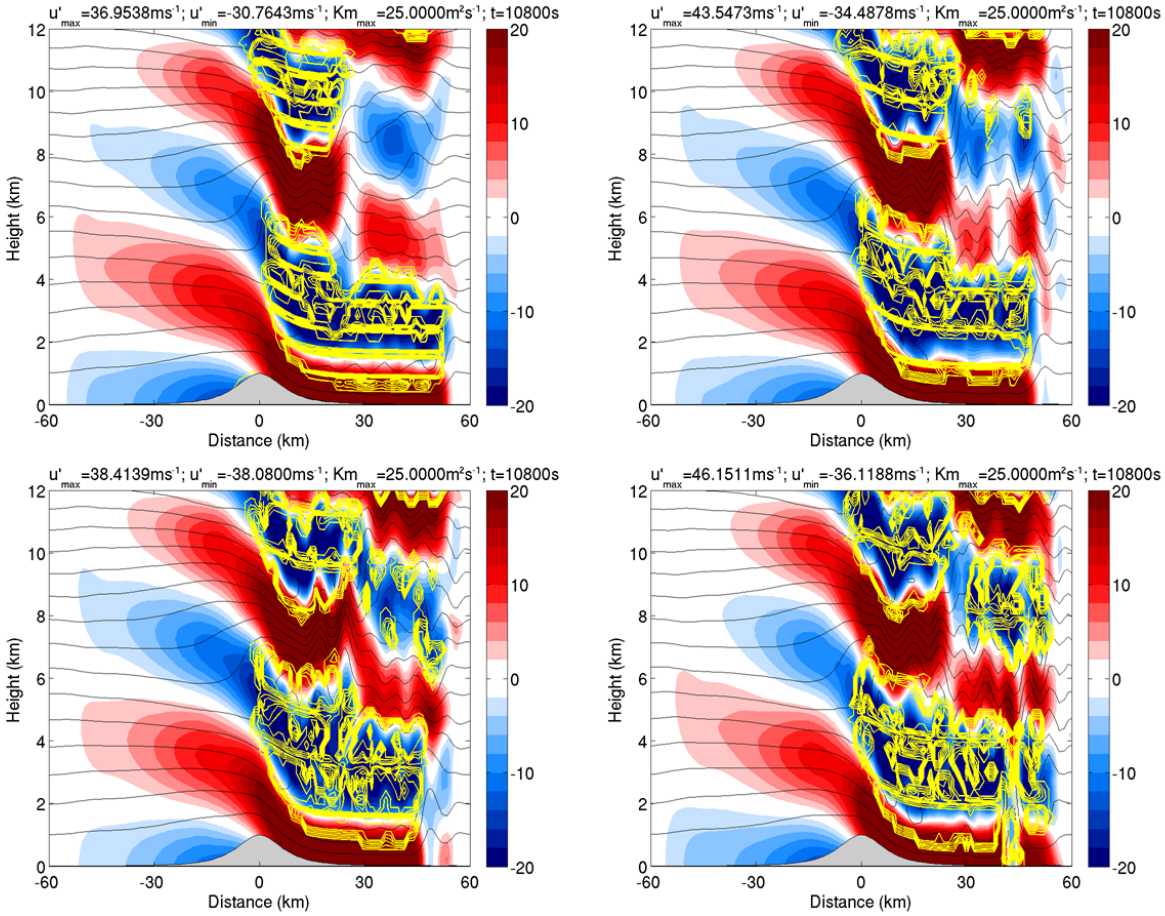

Figure 4: Same as Figure 3, except the effective grid scale is node-specific, limited by the vertical nodal spacing for all cases. The average nodal spacing is the same for all cases, the polynomial order of basis functions is p=4 (top left), p=6 (top right), p=8 (bottom left) and p=10 (bottom right).

The SE model with the physically parameterized subgrid-scale mixing was successfully tested for a nonlinear flow over an elongated mountain in three dimensions (Fig 5). The sloping isentropes in the lee of the obstacle are an indicator of wave breaking, which is evident in the non-zero values of the mixing coefficient. The computatioal domain was divided into 60 elements in both horizontal directions and the actual simulation was computed on 3600 computational cores (1 core per element).

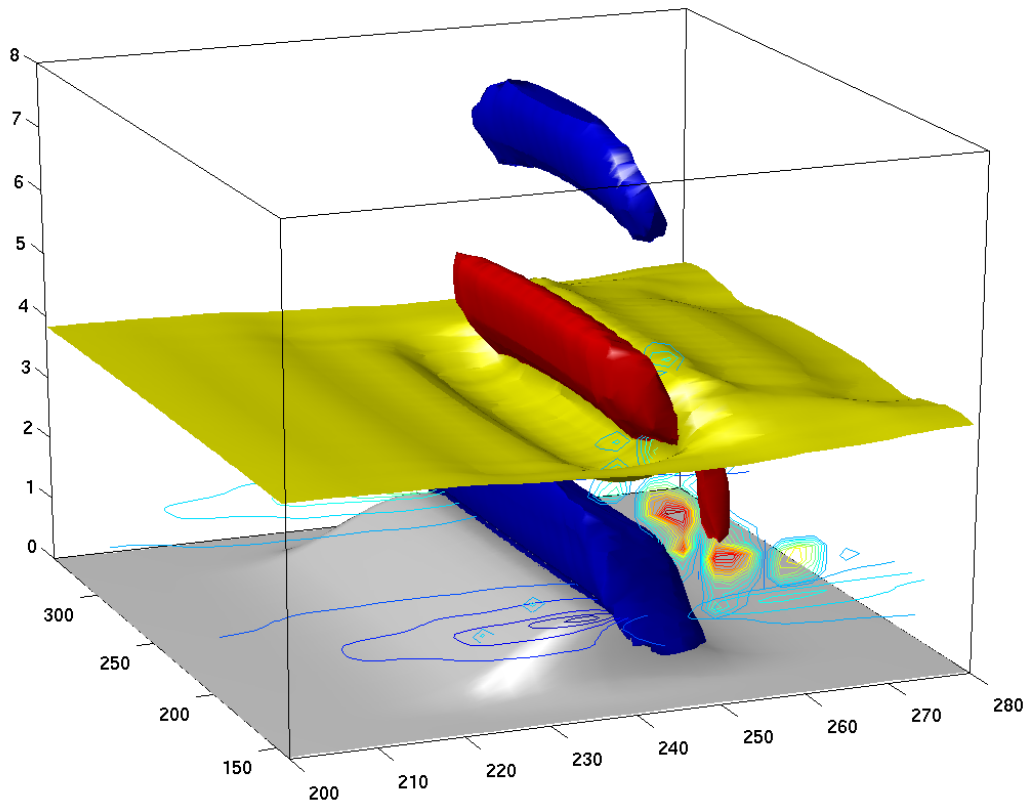

Figure 5: Flow over an elongated (cross-stream direction) ridge in three dimensions. The flow is from the left to right. Blue (red) isosurfaces represent positive (negative) vertical velocity of 2 (-2) ms-1. The isentropic surface of 290 K is yellow. Lateral flow deflection is depicted with colored contours in the x-y plane, while mixing is depicted with color contours in the x-z plane.

Gravity waves triggered by orography propagate vertically upwards, where they should exit the computational domain without spurious reflections. To achieve this, a top layer sponge is used in COAMPS with numerical damping. Large amplitude gravity waves require a larger damping coefficient to be effectively removed, but this in turn imposes an additional constraint on the maximaly stable time step. An implicit damping in the sponge layer (Klemp et al, 2008) has been implemented, which permits a larger damping coefficient and prevents crashes associated with stability constraints in the damping layer (Fig 7).

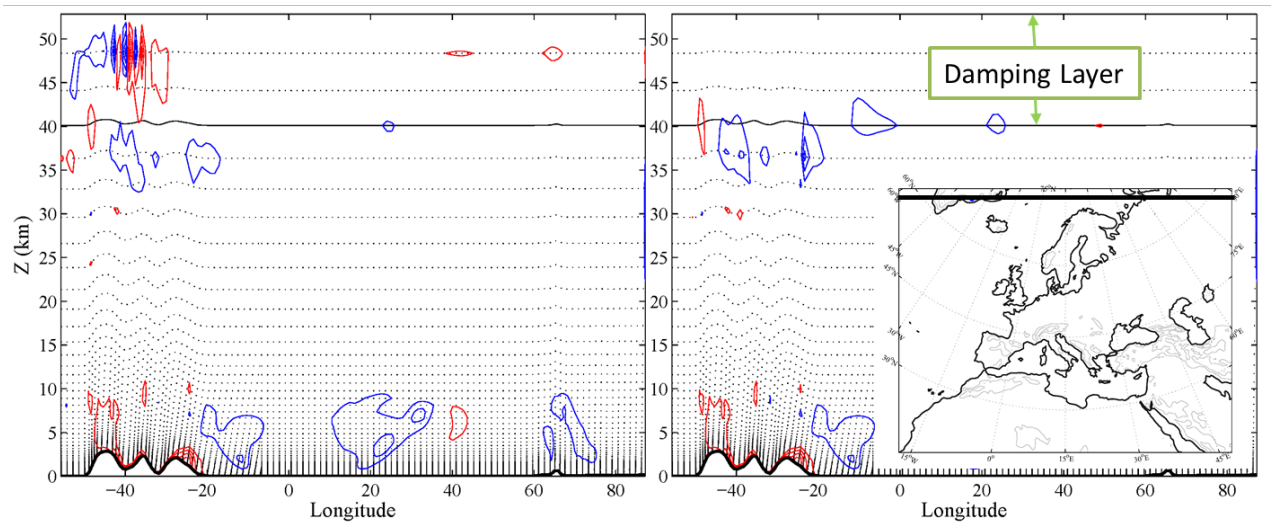

Figure 6: COAMPS forecast lead time t=18 hours, initialized at 00Z on 29th of November 2011, using NOGAPS initial and lateral boundary conditions. Vertical cross-section (indicated by a thick black line in the inset) of the vertical velocity with red (positive) and blue (negative) values, c.i. 0.05 ms^{-1}. Left panel with explicit and right panel with implicit damping.

IMPACT/APPLICATIONS

The SE model could become the unified dynamical core for both global and mesoscale weather forecasts across spatial and temporal scales for the US Navy. The design of the model and its structure yield excellent scalability that can take a full advantage of available computational cores as they become readily accessible in large numbers (~100000) in the near future.

COAMPS is the Navy's operational mesoscale NWP system and is recognized as the key model component driving a variety of DoD tactical decision aids. Accurate mesoscale prediction is considered an indispensable capability for defense and civilian applications. Skillful COAMPS predictions at resolutions less than 1 km will establish new capabilities for the support of the warfighter and Sea Power 21.

TRANSITIONS

The next generation COAMPS system will transition to 6.4 projects within PE 0603207N (SPAWAR, PMW-120) that focus on the transition COAMPS to FNMOC. The improvements to the COAMPS dynamical core have been transitioned to the SPAWAR 6.4 project and subsequently to operations as a result of the marked improvement in the geopotential height bias statistics.

RELATED PROJECTS

NUMA will be used in a related 6.2 project within PE 0602435 for an intercomparison of dynamical cores aimed at prediction across scales.

COAMPS will be used in related 6.1 projects within PE 0601153N that include studies of air-ice, air-ocean and air-wave coupling, boundary layer studies, and topographic flows and in related 6.2 projects within PE 0602435N that focus on the development of the atmospheric components (QC, analysis, initialization, and forecast model) of COAMPS.

PUBLICATIONS

Durran, D.R., and P.N. Blossey, 2012: Implicit-Explicit Multistep Methods for Fast-Wave Slow-Wave Problems, *Mon. Wea. Rev*., 140, 1307-1325 [published]

Gaberšek, S., J.D. Doyle and F.X. Giraldo, 2012: Dry and Moist Idealized Experiments With a Two-Dimensional Spectral Element Model, *Mon. Wea. Rev*., [in press]

Doyle, J.D., S. Gaberšek, Q. Jiang, L. Bernardet, J.M. Brown, A. Dörnbrack, E. Filaus, V. Grubišić, D. Kirshbaum, O. Knoth, S. Koch, I. M. Stiperski, S. Vosper, S. Zhong, 2011: An intercomparison of T-REX mountain wave simulations and implications for mesoscale predictability. *Mon. Wea. Rev*., 139, 2811-2831 [published]

Schmidli, J., B. J. Billings, F. K. Chow, J. D. Doyle, V. Grubisic, T. R. Holt, Q. Jiang, K. A. Lundquist, P. Sheridan, S. Vosper, S. F. J. De Wekker, C. D. Whiteman, A. A. Wyszogrodzki, G. Zaengl, 2011: Intercomparison of mesoscale model simulations of the daytime valley wind system, *Mon. Wea. Rev*., 139, 1389–1409 [published]